

Preparation and Characterization of Melamine–Formaldehyde–Polyvinylpyrrolidone Polymer Resin for Better Industrial Uses over Melamine Resins

Man Singh, Vinod Kumar

Chemistry Research Laboratory, Deshbandhu College, University of Delhi, New Delhi 110019, India

Received 31 July 2008; accepted 16 May 2009

DOI 10.1002/app.30805

Published online 24 June 2009 in Wiley InterScience (www.interscience.wiley.com).

ABSTRACT: Melamine–formaldehyde–polyvinylpyrrolidone (MFP) polymer resin was prepared with 1 : 16 : 1 ratios of melamine, formaldehyde (CH₂O), and polyvinylpyrrolidone amounts, respectively, by condensation polymerization at 6.9 pH. Structures were determined with IR, ¹H-NMR, and ¹³C-NMR spectroscopies. Chemical shifts (δ , ppm) were analyzed with singlet at δ 4.5, duplet from 3.13 to 3.17 and a quartet at 1.5 to 2.2 ppm for methylene (–CH₂–) bridging group, pyrrolidone, and polyvinyl constituents. The 3389.25, 1290.38, and 1655.28 cm⁻¹ stretching frequencies of –N=, –CH– and –C–O–O– groups, respectively, were noted on FTIR spectrum. The –C=N– melamine units reacted with CH₂O to adjoin with polyvinylpyrrolidone (PVP). An average viscosity molecular weight (M_v) 57,000 g mol⁻¹ was obtained with Mark–Hou-

wink–Sakurada equation. The chemical shift of –N(CH₂O)₂–C–pyrrolidone ring on ¹³C-NMR spectra was shifted toward lower magnetic field at 175.18 ppm. The resin was partially miscible with water thereby densities and viscosities of aqueous solutions were measured at 298.15 K temperature. It showed higher densities and viscosities than those of water. The resin developed exceptionally higher adhesive strength when its 62.29- μ m uniform thin film was applied on surfaces of wooden strips. The resin showed micellar behavior at about 0.009 g/100 mL aqueous solution. © 2009 Wiley Periodicals, Inc. *J Appl Polym Sci* 114: 1870–1878, 2009

Key words: average viscosity molecular weight; adhesive; stretching; frequencies

INTRODUCTION

Currently melamine has high significance in resin industries as it is frequently used for synthesis of several useful polymer resins. The melamine–formaldehyde and urea–formaldehyde and phenol formaldehyde and other several resins with various industrial uses are focused in science and technology,^{1,2} especially for textile³, paper, pulpwood, paints, and varnishes. The resins had occupied prime position and are widely used in industries⁴ as thickeners for several rheological applications in cosmetics, pharmaceuticals^{5,6} for bioprocessing⁷ and drug delivery systems.⁸ A substantial progress is being made for preparation of resins by condensation and ion exchange reactions⁹ for desired properties. The formaldehyde and melamine have been commonly used for several resin preparations but we have first time used the PVP as branching material along with formaldehyde and melamine. The PVP had introduced useful properties in the resins.^{9,1} The resins of formaldehyde and melamine

with the PVP have never been reported earlier. Thereby our work is considered to be of industrial significance in adhesive material technology. The melamine and PVP were bridged together with –CH₂– of formaldehyde and were illustrated with IR, ¹H-NMR, and ¹³C-NMR spectra. The detailed physicochemical properties on several aqueous PVP solutions were reported by Singh and Kumar.^{10,11}

This resin was noted highly cross-linked and translucent product with better adhesive strength and also a heat and moisture resistance than those of the reported resins.¹¹ It was biodegradable¹² and ecofriendly and may be used as a significant adhesive^{13–15} for paper binding and in the production of molding compounds, foams, and several other colloidal and emulsion industries. The MFP with lower concentrations of in the aqueous solutions worked as dilatant¹⁶ that increased a shear of viscosity but with increasing concentrations it worked as a pseudoplastic.¹⁷ A viscous flow of its solutions showed interesting variations with increase in concentrations due to thixotropic⁹ features. An adhesive strength of MFP was tested on paper, wood and molding compounds, and noted superior than of the others.¹⁸ A thin film of the resin was applied on smooth plywood surfaces to check its adhesive capacity where it showed an exceptional adhesive strength. The plywood had chemical composition as 50% cellulose,

Correspondence to: M. Singh (mansingh50@hotmail.com).

Contract grant sponsor: University Grants Commission, Govt. of India.

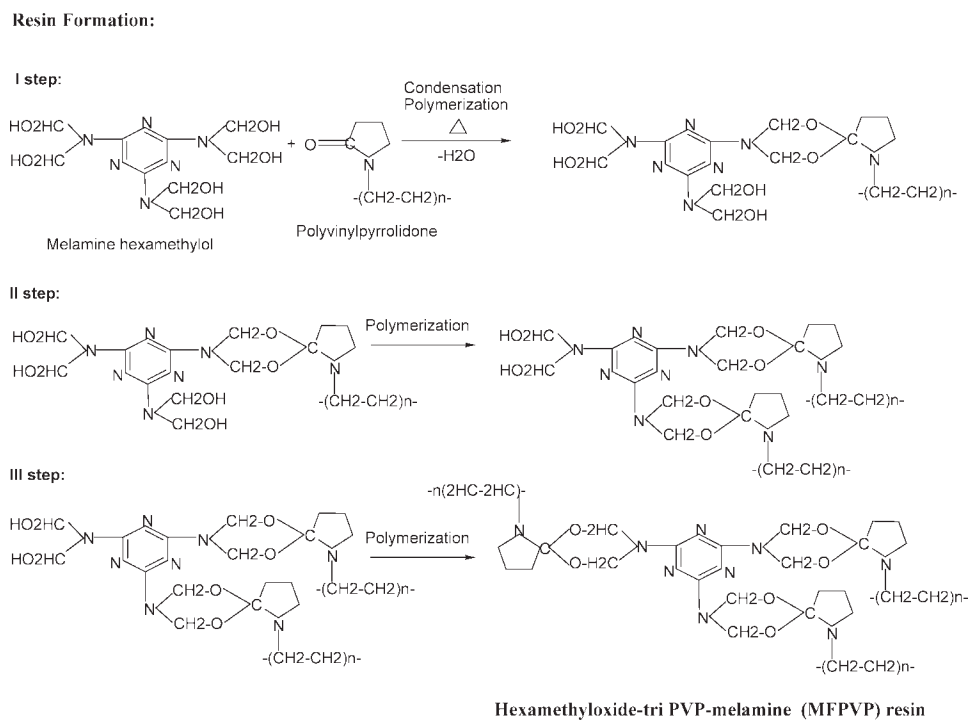


Figure 1 Resin formation: Hexamethyloxide-triPVP-melamine (MFPVP) resin.

15–30% hemicellulose, 15–35% lignin, 5–30% (w/w) ash, and extractives.¹⁸ In general, the resins are significantly used in plywood and paper pulp industries, and we tested our resin on plywood with highly encouraging results.

EXPERIMENTAL

The melamine (E. Merck, Mumbai, India; m.p. 300°C), formaldehyde 40% (E. Merck), and PVP (E. Merck; m.p. 165°C) were used for resin preparation with condensation process at 80°C with $\pm 0.1^\circ\text{C}$ temperature control for 3.30 h. First, the melamine was separately mixed with formaldehyde along with an addition of PVP in 1 : 16 : 1 mass ratios of melamine : formaldehyde : PVP in a 100-mL RB flask. Then the mixture was polymerized at 80°C for about 3.30 h, and the reaction was quenched in ice-cold bath. Then the product was extracted by placing the RB flask to normal temperature, and the condensation formed the MFP resin with 89% yield. The chemical reactions are illustrated in Figure 1; MFP for methylol and resin formation, respectively. The resin was stored in P_2O_5 vacuum desiccator. The pH showed negligible variation of ± 0.01 on condensation process as the formaldehyde, melamine, and polyvinylpyrrolidone did not dissociate, and no other protonic solvent was used as medium. Only the neutral water molecules were released and hence the pH remained as such.

Spectroscopy

An FTIR spectrum was recorded with a thin film within KBr disc with Nicollet Protégé-460 Spectrometer, and proton-NMR was monitored in deuterium on DPX-dix 300 MHz Bruker Avance spectrometer with TMS as an internal reference.

Physicochemical parameters

The resin solutions were prepared, w/v, with Millipore water and the densities with aqueous solutions (ρ_{aqs}) were measured² at 298.15 ± 0.05 K temperature control. Viscous flow times (t) and number of drops (n) for solution through a uniform capillary of 0.5 mm inner diameter were measured with Survisimeter¹⁹ (calibration no. 06070,582/1.01/C-0395; NPL, New Delhi, India) at constant temperature.⁴ The density of pure resin (ρ_r) was determined with 5-mL relative density bottle (RDB) and teflon cavity of 5 mL volumes.

Coating procedure

The resin sample was dried in a vacuum dryer for more than 6 h and the same was coated on the wood strip (WS) of 7.4 cm \times 2.8 cm area. The WS was dried for 48 h in hot air of 110°C in stainless steel chamber insulated with asbestos strips. After each 12 h during drying, the WS was kept in desiccator to attain normal temperature for weighing.

This exercise was repeated several times till a constant weight was noted. Then the resin was coated on the strip and kept in dried vacuum chamber. Both the WS and resin were kept in open to check air moisture absorption, and after each 8 h the moisture absorption was checked with weighing where no weight gain was noted. The moisture contents were also doubly ensured with anhydrous copper sulfate CuSO_4 which did not show color changes with resin. Thus, the resin was nonhygroscopic and a uniform coating of the resin on the WS was made by chromatographic glass slide. The weight of coated resin was determined by deducting a weight of WS before and after coating, which was 0.10137 g.

Densities

The densities were determined by filling the resin in 5-mL RDB and in another RDB of similar capacity, the water was filled as reference liquid to same level of the RDB as of the resin. The weights of the empty RDB (W_e), with resin (W_r) and water (W_w) filled were determined. The densities were determined with eq. (1).

$$\rho_r = [((W_r - W_e)/(W_w - W_e)) + 0.0012(1 - ((W_r - W_e)/(W_w - W_e)))]\rho_w \quad (1)$$

The ρ_r and ρ_w are densities of resin and water, 0.0012 is air density, and $(1 - ((W_r - W_e)/(W_w - W_e)))$ is a buoyancy correction in weights in air. The measurements were repeated with a fixed volume cavity of Teflon (TC), a nonsticking material, and the TC was absolutely dried by keeping in P_2O_5 filled dessicator for 24 h. Then the TC was weighed and its volume was determined by filling known volume of water which was measured with calibrated microburette. A freshly prepared resin was filled in TC and weighed, and the ρ_r was calculated eq. (2).

$$\rho_r = W_r/V_r \quad (2)$$

The V_r volume and W_r , the weight of the resin, the W_r was calculated from $W_{\text{TCr}} - W_{\text{TC}}$ where the W_{TCr} the weight of TC plus resin and W_{TC} is weight of TC only. The ρ_r of MFP resin with both the methods were 0.7798 g cm^{-3} or $0.7798 \times 10^{-3} \text{ kg m}^{-3}$, with a negligible difference in both the values.

RESULTS AND DISCUSSION

Resin coating thickness (RCT = t): The volume of a spreaded resin v_r .

The weight of the resin coated on the WS was determined, and the volume was calculated with eq. (3).

$$v_r = m_r/\rho_r \quad (3)$$

The m_r , v_r , and ρ_r are spreaded mass, volume, and density of resin; the v_r of resin spreaded on the WS was calculated as follows:

$$v_r = l \times w \times t \quad (4)$$

The l is length, w is width of WS, and the t is coating thickness of the resin. The $l = 7.4 \text{ cm}$, $w = 2.8 \text{ cm}$, and t is unknown and was determined with eq. (5).

$$v_r = (7.4 \text{ cm})(2.8 \text{ cm})(t \text{ cm}) \quad (5)$$

$$v_r = 20.72t \text{ cm}^3 \quad (6)$$

Similarly the m_r was determined by deducting the weight of the resin uncoated WS from the coated WS, and was 0.1014 g. Thus with the $\rho_r = 0.7798 \text{ g cm}^{-3}$, $m_r = 0.1014 \text{ g}$ values, the t was calculated with eq. 3 taking the v_r values from eq. 6 and was $20.72t \text{ cm}^3 = (0.1014 \text{ g})/(0.7798 \text{ g cm}^{-3})$. The $t = 0.00627 \text{ cm} = 0.00627 \times 10^{-2} \text{ m} = 62.74 \mu\text{m}$ ($62.74 \times 10^{-6} \text{ m}$) was obtained and held at 57-N force by hanging weights with spring balance.

Weight holding capacity

The resin held 57-N force with higher WHC (Table I) where a cross-linking in the resin enhanced an adhesiveness when compared with a similar resin prepared at 40°C that held 13.3 N force. Hence the WHC is a direct function of cross-linking. The weights which were hung were calibrated at NPL. The density (ρ) was 1.0009 g cm^{-3} and of a RCT was $62.69 \mu\text{m}$.

Molecular weight determination

Size and shape dependence of viscosity of a macromolecule was used for molecular weight determinations. The viscous flow times for both the solvent and dilute resin solutions were measured with survismeter for viscosities. Relative viscosities (η_r) were calculated with eq. (7).

$$\eta_r = \eta/\eta_0 = (\rho t)/(t_0 \rho_0) \quad (7)$$

TABLE I
Densities ρ ($\times 10^3 \text{ kg m}^{-3}$ with $\pm 2.4 \times 10^{-2} \text{ kg m}^{-3}$ Standard Error, $t \pm 10^{-2} \text{ s}$), Viscosity η ($\pm 4 \times 10^{-5} \text{ N s m}^{-2}$), and Surface Tension γ (mN m^{-1})

Concentration (mg %)	ρ	η	γ
11	1.00091	1.0014	69.397
9	1.00050	1.0033	68.026
7	0.99961	0.9923	69.765
5	0.99873	0.8360	70.169
3	0.99788	1.0154	70.580
1	0.99699	1.0044	70.993

The η and η_0 are viscosities of solution and solvent, t and t_0 flow times and ρ and ρ_0 are densities of solution and water, respectively. The data are given in Table I. The ρ data were determined with weight method reported in our earlier article.¹⁰ Absolute distributions of molecular weights could be studied with group analysis¹³ and osmometry.²⁰ But intrinsic viscosity $[\eta]$ was noted to be an effective technique for average viscosity molecular $[\bar{M}_v]$. The $[\eta]$ derived from η_r and were fitted to Mark–Houwink–Sakurada equation.¹¹ The specific ($\eta_{sp} = (\eta_r - 1)$) and reduced viscosities ($\eta_{red} = ((\eta_r - 1)/c)$) were determined and plotted against concentrations as eq. (8).

$$\eta_{red} = \eta_{sp}/c = [\eta] + Dc \quad (8)$$

The η_{sp}/c , at $c \rightarrow 0$, is intrinsic viscosity $[\eta]$ and D is a slope, the six dilute solutions of MFP were prepared for $[\eta]$ data and fitted in $(\log [\eta] = \log k + a \log M)$ relation. Different molecular weights of PVOH were used as markers¹¹ for $(k$ and $a)$ constants determination of above relation. The $\bar{M}_v = 56,990 \text{ g mol}^{-1}$ was noted for our resin sample. The molecular shape was derived with the following Einstein equation.²¹

$$(\eta_r = \eta/\eta_0) = 2.5v/V \quad (9)$$

The v/V data were lower than 2.5 because of spherical shape of the MFP. The relation of η/η_0 with 2.5 v/V term was given by Einstein²¹ for ensuring shape and size of the polymeric materials. Our data inferred a spherical shape where the resin had grown in cross-linked structure as the PVP units favor further polymerization with many free vinyl chains. The longer vinyl chains due to induction and steric effects do cause some attachments inside the resin molecule. So the cross-linking is possible. The rate (R) of surface tension variation with increase in concentration c was calculated with eq. (10).

$$R = (d\gamma/dc)_{T,P} = \gamma_2 - \gamma_1/c_2 - c_1 \quad (10)$$

The R is rate of surface tension (γ_1 and γ_2) and (c_1 and c_2) are pre and post surface tension and concentrations of the MPF resin, respectively.

The viscosities increased with increase in concentration but at 5 mg % the viscosities tremendously decreased and then again increased at an equal rate. It may be due to higher solvation at 5 mg %, and this amount is noted as critical concentration (CC) with formation of molecular colloids enclosing the water molecules in interstitial void spaces of the resin molecule.

A shear rate increased at the CC with molecular geometry of a resin with Newtonian and non-New-

tonian flow behaviors with specific solute–solvent interactions. Perhaps at the CC, the higher number of water molecules entered interstices with higher hydrodynamic volume with higher internal pressure. Perhaps the water molecules were expelled out from interstices to bulk water because of an internal molecular structure of the MFP resin. The viscosities decreased because of weakening in both the cross-linking and shear that inferred a weakening in both the interactions and hydrogen bonding capacities. A smaller sized MFP resin molecule with maximum asymmetry and stronger interaction exists in optimized state. The MFP contains 9 nitrogen atoms (Fig. 1) with loan pair of electrons that facilitated its interaction with cellulose of wood used as a base surface for the coating.

Weight holding capacity

The number of N-atoms increased the WHC strongly with higher adhesive forces, for example resin with 9 N-atoms causes stronger adhesive forces and held 30 kg weight. The viscosities inferred stronger shear with higher γ values. The γ values decreased for 6.8 mg % with same @ of decrease but from 6.8 to 8.8 mg %, the @ of decrease of surface tension was higher (Fig. 6). But from 8.8 to 10.8 mg % concentrations, the γ values increased and the η values also increased for 0.8 mg % with same @ but from 2.8 to 4.8 mg %, the @ decreases in the values was higher. However, from 4.8 to 6.8 mg % the η values increased with stronger resin interactions with water.

The PVP was water soluble, and, thus, it introduced an element of degradability in our polymer resin. The PVP was connected with —N— atom of melamine via $\text{—CH}_2\text{—}$ of CH_2O , the formaldehyde and O=C— (ketonic) group of PVP with itself. The O of the O=C— had undergone an electronic change for an attachment with N atom of melamine (Fig. 1). So the resin action mechanism was noted sharper and useful in comparison to routinely used resins.

IR spectra

Stretching frequencies at 3389.25, 2965.95, 2912.57 cm^{-1} vibrations infer —N= tertiary amine, and —CH_2 groups of $\text{—(CH}_2\text{—CH}_2)_n$ vinyl chain of the PVP, respectively (Fig. 2). A new band at 2362.17 cm^{-1} inferred a —CH_2 of formaldehyde attached with O atoms of PVP in the resin. A frequency at 1655.28 cm^{-1} showed a partial ketonic group (=C=O) of PVP where its O atom was not removed except certain electronic reorientations. The partially ketonic group with =C—N of PVP and $\text{—CH}_2\text{—CH}_2\text{—}$ chain of formaldehyde induced stretching frequency at 1655.28 cm^{-1} of =C—O—O—

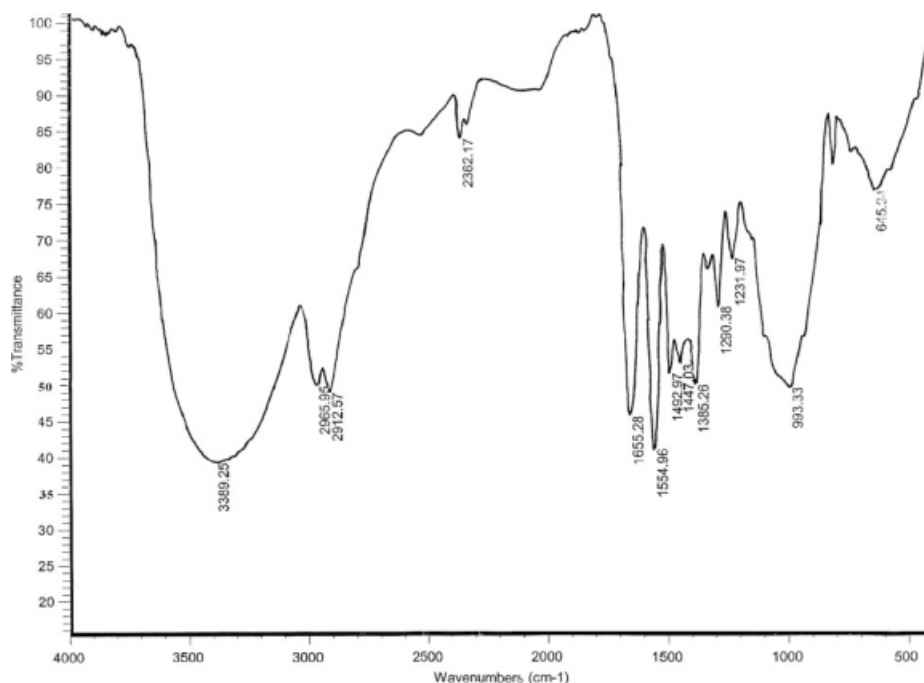


Figure 2 IR of MFP resin.

with a weaker ketonic character. The frequency at 1554.96 cm^{-1} infer $=\text{C}=\text{N}-$ of a melamine ring. Further, a bending at 1492.97 , 993.33 , 645.94 cm^{-1} denoted the C—H bending and C—H out of plane deformation, respectively. The bending at 1385.26 cm^{-1} inferred a doublet of the $-\text{CH}_2-$ of the PVP ring in the resin, and a bend at 815.05 cm^{-1} was noted because of $=\text{N}-$ stretching of PVP in the ring. A stretching frequency at 1290 cm^{-1} inferred symmetric and asymmetric $-\text{C}-\text{O}$ groups, with an absence of carbonyl group. The 1447.03 cm^{-1} stretching frequency depicted a deformed position of the $-\text{CH}_2-$ between $-\text{N}=\text{C}-$ functional groups of the melamine and PVP in the resin molecule. The CH_2O reacted with both the H atoms of $-\text{NH}_2$ to furnish a $-\text{CH}_2-$ where an electron density of the $-\text{CH}_2-$ was disrupted by N atom of melamine and the $-\text{C}$ of $-\text{C}=\text{O}$ group of the PVP. The O atom with higher electronegativity attracted a shared pair of electron from PVP unit to enable the O to develop a bond with N of melamine and C atoms of PVP with the two $-\text{CH}_2-$ of the formaldehyde. The stretching frequency at 1385.26 cm^{-1} was noted for a symmetric $-\text{CH}_2-$ of the PVP chain. An absence of band between 1700 and 1800 cm^{-1} inferred a partial conversion of $-\text{C}=\text{O}$ of PVP into $-\text{C}-\text{O}-\text{O}-$. The MFP showed a frequency at 2362.17 cm^{-1} because of a bridged $-\text{CH}_2-$ and the bands at 1492 , 993 , 645 cm^{-1} inferred the C—H bending and C—H out of plane deformations. The 1554.96 cm^{-1} stretching was of the melamine ring, the 1231.97 cm^{-1} stretching was for out of plane because of a weak overtone.

A combination of bonds in a region of 1554.96 and 1290.38 cm^{-1} stretching for the $-\text{C}-\text{O}$ group, the 2362.17 cm^{-1} stretching was for $-\text{CH}_2-$ group. Since N atom was electron withdrawing and attracted electron pair of O atom toward its own side.

IR spectra of MFP differs than of the MUF resins

The MUF showed a sharper band at 3330 cm^{-1} but the MFP at 3389.25 cm^{-1} showed a broad (Fig. 2) band¹⁸ because of stronger hydrogen bond. The MUF at 3330 cm^{-1} showed a superimposition of stretching vibration of $-\text{OH}$ with the $=\text{NH}$ vibration. With the MUF, at three sides the N atoms were attached to $-\text{CH}_2-$ but with the MFP, an attachment is with $-\text{O}-$ and $-\text{CH}_2-$. It made a difference in IR stretching of $\equiv\text{C}-\text{N}=\text{C}-\text{O}-\text{O}-$ but the MUF showed a symmetry stretching. The MFP caused asymmetric stretching, and a Fermi resonance was noted stronger with MFP as band occurred at 1655.28 cm^{-1} because of the Fermi resonance where a mutual perturbation was noted at 1447.03 cm^{-1} sharing a bond at 1385.26 and 1290.38 cm^{-1} . But the MUF did not show Fermi resonance in this region because of a greater symmetry in the structure.¹⁸ Also the MFP was a asymmetric structure in (Fig. 3), the $-\text{CH}_2-(\text{C}-\text{H})$ in MFP was due to Fermi resonance that caused a band at 2912.67 cm^{-1} against 2820 cm^{-1} . However, in case of the MUF, it was at 2654 cm^{-1} , further the frequency of $(\text{C}-\text{H})$ was lowered because it interacted with $-\text{O}-$ group.

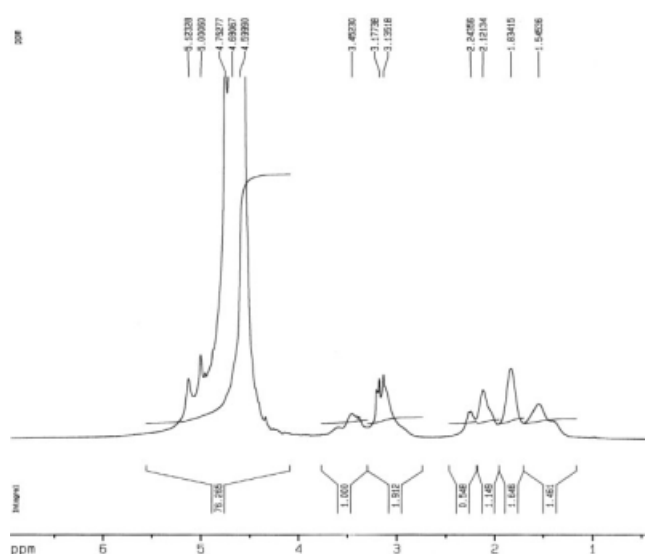


Figure 3 Proton-NMR spectrum for MFP resin.

Hence the MFP caused the vibration frequencies at 2965.95 and 2912.57 cm^{-1} . The $-\text{CH}_2-$ of the MFP showed mesomeric effect because of the different environment in the molecule while the MUF¹⁸ did not do so because of a simpler structure when compared with our MFP resin.

¹H-NMR spectra

The ¹H-NMR was recorded in CDCl_3 , and depicted attachments of N of $-\text{NH}_2$ of melamine and of $=\text{C}=\text{N}$ of PVP with $-\text{O}-$ and $-\text{CH}_2-$. The NMR was monitored in deuterium on DPX-dix 300 MHz Bruker Advance spectrometer using TMS an internal reference. The proton-NMR is reported in Figure 3, and depicted that the melamine with $-\text{O}-$ and $-\text{CH}_2-$ in the form epoxide responded at a low magnetic field. On condensation, an electron density of bridged carbon signals was at 3.4–3.1 ppm because the duplet was attributed to a field effect of neighboring nitrogen atom which was electron deficient. A field shift to 4.5 ppm was assigned to a singlet of $-\text{NH}_2$ group as the condensation of the melamine nucleus with polyvinylpyrrolidone and formaldehyde shifted an electron density to a lower field. The quartet at 2.2–1.5 ppm was due to a merging of the $-\text{CH}_2-$ of the pyrrolidine ring and $-\text{CH}_2-$ of the vinyl chain.

The H of bridged $-\text{CH}_2-$ responded to slightly lower magnetic field from 4.5, 4.6, 4.7, 5.0, and 5.1 ppm, because of N and C atoms with different electron densities. It showed a critical splitting of H of the $-\text{CH}_2-$. A splitting singlet at δ 4.5 ppm, duplet at δ 3.1–3.17 and a quartet at δ 1.5–2.2 ppm analyzed protons position of $-\text{CH}_2-$ bridging groups. A stability of the $-\text{C}-\text{H}$ bond of $-\text{CH}_2-$ was lowered by heteroatomic environments and its $-\text{C}-\text{H}$ split at

lower magnetic fields i.e., 4.5–5.1 ppm. The $=\text{CH}_2$ of PVP was slightly in a similar environment except C i.e., attached to $-\text{CH}_2-$ and the O atom of bridged. It split the $=\text{CH}_2$ at 3.1, 3.2, and 3.4 ppm, a higher field than of a bridged $-\text{CH}_2-$ group. The $=\text{CH}_2$ at one side was linked with C of the PVP and another side with N atom of a melamine, opposing O atom. It split into three different chemical shifts.

¹³C-NMR spectra

The ¹³C-NMR spectrum was obtained with Bruker 300 MHz Spectrometer with $\text{DMSO}-d_6$ a nondeuterated internal standard and signals at 40.36–38.69 ppm were for DMSO solvent. The spectrum is shown in Figure 4(a,b) and chemical shifts are given in Table II, in this context the substitution of H_2 of $=\text{C}-\text{NH}_2$ of melamine by CH_2O of a binder reported the signals at a lower field between 93.61 and 92.35 ppm. The $-\text{CH}_3$, $-\text{CH}_2-$, $-\text{C}-\text{O}-\text{O}-$, $-\text{N}-\text{CH}_2-$ $\text{O}-\text{C}<$ groups, and $-\text{C}-\text{C}-$ of pyrrolidone quartet were at high fields. An electron density of C atom of melamine, $-\text{C}-\text{N}=\text{C}$ and $-\text{N}-\text{CH}_2-$ attached with $\text{PVP}-\text{C}=\text{O}$ group with respective signals at 93.61, 92.35, and 89.90 ppm, respectively. The PVP is a copolymer with non propagating $-(\text{CH}_2-\text{CH})_n-$ chains and melamine with substituted groups split at a low magnetic fields. The signals at 93.61, 92.35, and 89.90 ppm are for carbon atoms of the melamine and the $-\text{CH}_2-$ of PVP at 89.90 ppm, while the $=\text{C}-\text{N}$ and $-\text{N}-\text{CH}_2$ groups appeared at 88.22 ppm with split [Table II and Fig. 4(b)]. The signals at 87.03 and 82.36 ppm occur because of $-\text{C}-\text{N}$ groups (PVP) split. The vinyl chain $-(\text{CH}=\text{CH}_2)_n-$ of the PVP appeared at 85.53 and 85.36 ppm [Fig. 5(b)] showed the signals for C atom of PVP. The three active zones are noticed in ¹³C-NMR spectra with chemical shifts at high field for vinyl chain. The signals at 55.71 to 55.39,

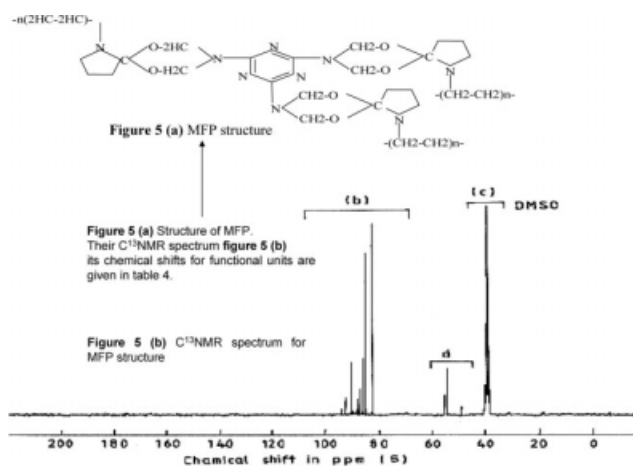


Figure 4 Structure and ¹³C-NMR spectra of the MFP resin.

TABLE II
Chemical Shifts of ^{13}C -NMR Spectra of MFP Resin of Figure 3(a,b)

Figures	Bands	Structural units	Structural units	δ (ppm)
3(b)	1	Melamine	$\equiv\text{C}-\text{N}$	93.61 to 92.35
	2	PVP	$-\text{N}-\text{CH}_2-$	89.90
	3	Melamine splitting	$\equiv\text{C}-\text{N}$	88.22
	4	PVP splitting	$\text{N}-\text{CH}_2-$	87.95
	5	PVP ring	$\equiv\text{C}-\text{N}-$	87.03
	6	PVP ring	$-\text{N}-\text{CH}_2$	85.80
	7	Vinyl chain	$-(\text{CH}_2-\text{CH}_2)_n-$	85.53
	8	Vinyl chain	$-(\text{CH}_2-\text{CH}_2)_n-$	85.36
	9	PVP vinyl chain	$-\text{CH}_2-\text{CH}_2-$	84.70
	10	PVP vinyl chain	$-\text{C}-\text{N}-$	82.36
	11	Pyrrolidone ring	$-\text{O}-\text{C}=\text{}$	92.35
3(c)	1	Quartet C atom, PVP	$=\text{C}=\text{}$	55.71 to 55.39
	2	C of $-\text{CH}_2-$ between N and O	$-\text{N}=[\text{CH}_2-\text{O}]_2-\text{C}=\text{}$	54.47
	3	C of $-\text{CH}_2-$ between O and C	$\text{O}-\text{CH}_2-\text{C}=\text{}$	49.11
3(d)	1	DMSO	$(\text{CH}_3)_2\text{SO}$	40.36 to 38.69
	2	$-\text{CH}_2-$ group	$-\text{CH}_2-$	31.47
	3	Terminal $-\text{CH}_3$ of vinyl chain	$-\text{CH}_3$	18.38

54.47, and 49.11 ppm were due to $=\text{C}=\text{}$ quartet C atom of PVP ring. The signal at 49.11 ppm $-\text{CH}_2-\text{O}-$ of the bridge, the signal 82.36 ppm at $-\text{C}-\text{N}$ of the melamine and the 84.70 ppm is for $-\text{CH}_2$ vinyl chain of the PVP, the 54.47 ppm $-\text{C}-\text{O}$ of the PVP ring.

Melamine ring in resin molecule

The $-\text{N}-\text{CH}_2$ in the resin product is surrounded by the $\text{N}-(\text{CH}_2-\text{O})_2-\text{C}$ -pyrrolidone ring of the PVP with a total distortion of a symmetric electron density distribution of the $-\text{NH}_2$ and electron density of the C of the melamine ring (Fig. 5). The melamine ring in the resin macromolecule occupied a center-most location referred to as a core²². An expression

of the C atom of the melamine ring at core is totally shattered as the ring is embedded in the deepest zone with respect to the growth of the resin with $\text{N}-(\text{CH}_2-\text{O})_2-\text{C}$ -pyrrolidone ring which acts as dendrimer units²³. The O atom of the $-\text{N}-(\text{CH}_2-\text{O})_2-\text{C}$ -pyrrolidone ring also influenced the C electron density. These distortions in the melamine core ring reduce intensity of the band of the C atom and pushed its weaker pulse at 175.18 ppm [Fig. 5(e)]. Thus, the melamine actively take part in the resin formation but its original band at 167 ppm is located to a weak filed at 175.18 ppm rather than 167 ppm. Thus, an inhibition in an expression of the ^{13}C -NMR response of the C atom of the bound melamine is considerably disrupted. Thus our structural propositions in Figure 4(b) supported by electronic

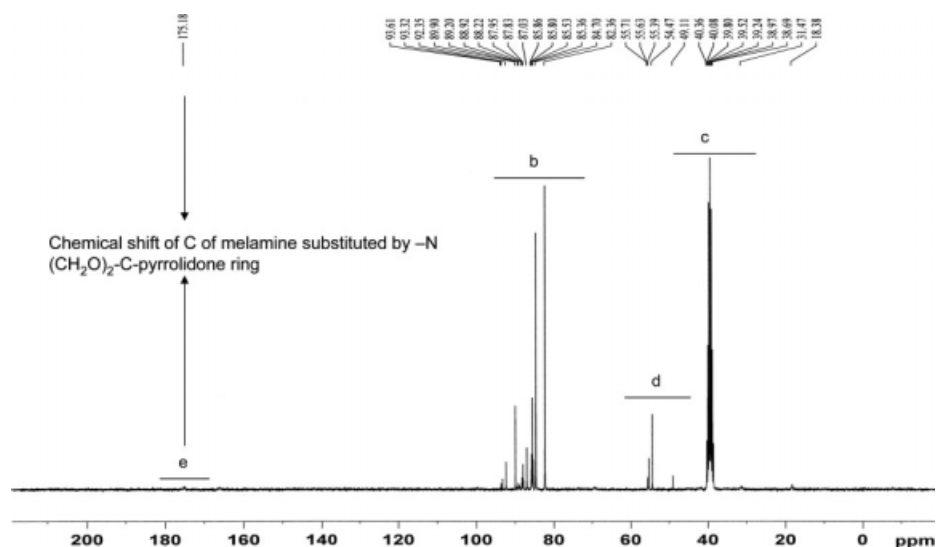


Figure 5 The chemical shift of C atom of the melamine ring in resin molecule.

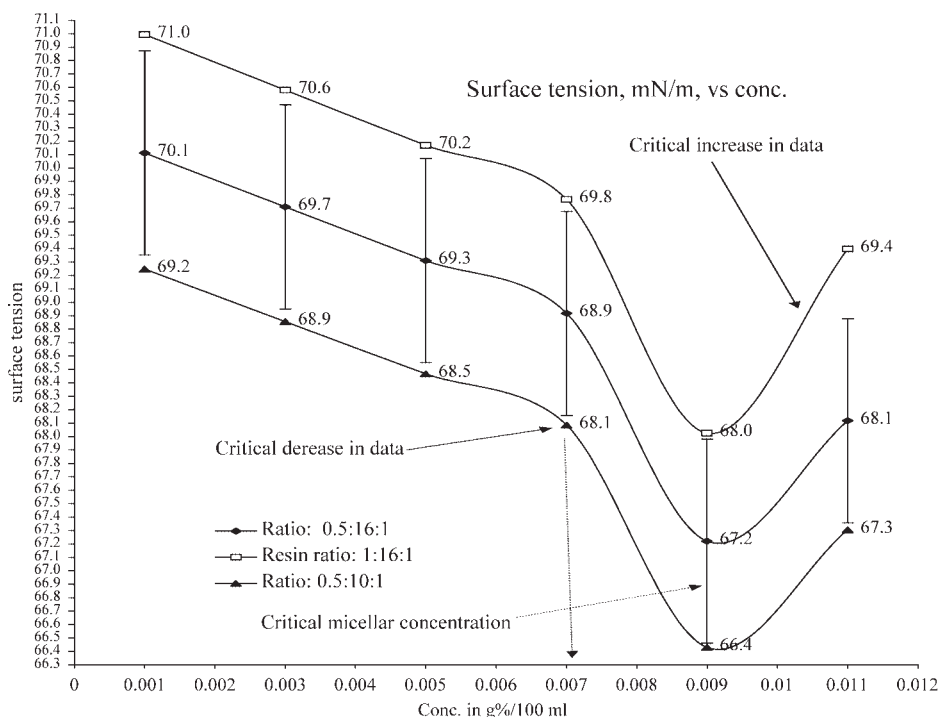


Figure 6 Surface tension and concentration of MFP resin.

distortion and much assymetricity in structures which could denoted as supramolecular structures. Thus, the stoichiometric elemental relationship of the polymer product is correctly denoted in Figure 2. Further a mild solubility of our resin product with water denied a formation of the melamine–formaldehyde reaction products because such products are insoluble in most organic solvents including water. This inferred a presence of the $-\text{N}-(\text{CH}_2-\text{O})_2-\text{C}-$ pyrrolidone ring that is responsible for weaker solubility in water. The $-\text{N}=\text{C}$ amine group has shown chemical shift at 175.18 ppm [Fig. 5(e)] because the $\text{C}-\text{C}$ bond of melamine experienced the force of the $-\text{N}-(\text{CH}_2-\text{O})_2-\text{C}-$ pyrrolidone unit in place of the H atoms of the original melamine molecules. These substitutions have weakened the $\text{C}-\text{C}$ bond strength in the resin macromolecule. Thus, the chemical shift is shifted toward lower magnetic field at 175.18 ppm. The 167.4 ppm is shown by C in the $\text{C}-\text{C}$ bond attached with $-\text{NH}_2$ but when H atom is substituted by $-\text{N}-(\text{CH}_2-\text{O})_2-\text{C}-$ pyrrolidone unit. The stretching frequency is lowered to 3389 cm^{-1} but for unsubstituted melamine this frequency is 3470 cm^{-1} . Thereby the $-\text{NH}_2$ group environment is changed because of replacement by the $-\text{N}-(\text{CH}_2-\text{O})_2-\text{C}-$ pyrrolidone. The FTIR (Fig. 3) showed change in stretching frequencies of $-\text{NH}_2$ of the melamine attached to its carbon atom in the form of the $\text{mel-C}-\text{NH}_2$. So the chemical shift of C of melamine in substituted environment is denoted with 75.18 ppm. Thereby the ^{13}C -NMR and FTIR

spectra did infer a presence of the melamine ring in the resin preparation.

Surface properties

The surface tensions of resin (1 : 16 : 1) along with other samples of 0.5 : 16 : 1 and 0.5 : 10 : 1 ratios of the melamine, formaldehyde and PVP, respectively, are noted as (1 : 16 : 1) > (0.5 : 16 : 1) > (0.5 : 10 : 1) (Fig. 6). The surface tension of water is 72.14 mN m^{-1} with stronger dipolar interactions while the surface tension of the *n*-hexane is 17.90 mN m^{-1} with the weaker interactions. Thus the higher surface tension of our polymer resin with water showed stronger water–resin interactions but a lower surface tension with weaker interactions. Comparatively our resin showed a lower surface tension than of the water with a decreasing trend with increasing compositions with weaker dipolar interactions. Thus, the resin compositions weaken the resin–water interactions with 2 mN m^{-1} decrease in surface tension. The surface tensions decreased from 69.2 to 68.9 for 0.001–0.003, 68.9 to 68.5 for 0.003–0.005, 68.5 to 68.1 for 0.005–0.007, 68.1 to 66.4 mN m^{-1} for 0.007–0.009 with increase from 66.4 to 67.3 mN m^{-1} for 0.009–0.011 mg % resin. A decrease in surface tension with increasing concentration defines a stronger weakening in dipolar interaction. The surface tensions of resins of 0.5 : 16 : 1, 0.5 : 10 : 1, and 1 : 16 : 1 inferred that with higher CH_2O ratio caused a higher cross-linking. Thus, the resin disrupted the

water structure mildly when compared with resin with lower CH₂O ratio, and with this resin, the cross-linking is of lower level that strongly destabilized the water structure. But the resin with 1.0 : 16 : 1 ratio produced the surface tensions between 0.5 : 16 : 1, 0.5 : 10 : 1 and 1 : 16 : 1 ratio samples with 0.9 mN m⁻¹ higher and 0.9 mN m⁻¹ surface tensions. Thus our resin with optimum surface tension was studied. All the three samples showed drastic decrease in surface tensions at 0.007 mg % and @ of -157.9 mN m⁻¹ but the @ of decreased from 0.0075 to 0.009 is -850 mN m⁻¹ but surface tensions increase from 0.009 to 0.011 @ 450 mN m⁻¹. These decrease and increase in the @ remain same for the samples. This similarity in the @ defined a similar mechanism of the interaction. Further from 0.007 to 0.009 is 5.4 time higher decrease than of a previous @ of decrease. However, an increase in the surface tension data from 0.009 to 0.011 is 1.9 times lower than of the 0.007 to 0.009 mg %. Thus, the resins decreased surface tension because of void volumes or interstices inside resin molecule where the water structure entered in void volumes. The PVP units acted as dendrimer units and disrupted the hydrogen bonding of the water. This process of interaction continued to decrease the surface tensions but a solvation process comes at 0.007 where again intermolecular forces on surfaces redistribute. The drastic reorientations with maximum change with entangled water molecules with a maximum decreased in surface tension occurred. This structure at about 0.009% onwards tried to regain the resin-water interaction with an increase in surface tension.

CONCLUSION

The MFP resin was noted spherical in shape with 57×10^3 g mol⁻¹ viscosity average molecular weight (\overline{M}_v). The adhesive strength of the resin increased with degree of cross-linking which increased with temperature during sample preparations. The

aqueous resin solutions were noted non-Newtonian solutions with shear stress on laminar flow. The surface tension of the resin decreased with increase in concentrations with formation of the micelles at 0.009 g %.

The authors are thankful to Dr. A.P. Raste, Principal, DBC, for infrastructural support.

REFERENCES

1. Liang, L.; Xu, Y.; Zhang, L.; Sheng, Y.; Wu, D.; Sun, Y. *J Opt Soc Am B* 2007, 24, 1066.
2. Collinson, M. M. *Crit Rev Anal Chem* 1999, 29, 289.
3. Miksik, I.; Deyl, Z. *J Chromatogr B Biomed Sci Appl* 2000, 739, 109.
4. Bielawski, C. W.; Grubbs, R. H. *Prog Polym Sci* 2007, 32, 1.
5. Shi, L.; Miller, C.; Caldwell, K. D.; Valint, P. *Colloids Surf B: Biointerfaces* 1999, 15, 303.
6. Bakshi, M. S.; Kaura, A.; Kaur, G. *J Colloid Interface Sci* 2006, 296, 370.
7. Chen, G.; Jing, W.; Xiangfeng, L.; Lili, Z.; Huizhou, L. *Sci China Ser B: Chem* 2006, 49, 541.
8. Determan, M. D.; Cox, J. P.; Seifert, S.; Thiagarajan, P.; Mallapragada, S. K. *Polymer* 2005, 46, 6933.
9. Poljansek, I.; Krajnc, M. *Acta Chim Slov* 2005, 52, 238.
10. Singh, M.; Kumar, S. *J Appl Polym Sci* 2004, 87, 1001.
11. Singh, M. *Ind J Chem* 2004, 43, 1696.
12. Dontulwar, J. R.; Borikar, D. K.; Gogte, B. B. *Carbohydr Polym* 2006, 63, 375.
13. Benard, Q.; Fois, M.; Grisel, M.; Laurens, P. *Int J Adhes Adhesives* 2006, 26, 543.
14. Nakayama, M.; Okano, T.; Miyazaki, T.; Kohori, F.; Sakai, K.; Yokoyama, M. *J Controlled Release* 2006, 115, 46.
15. Yim, M. J.; Paik, K. W. *Int J Adhes Adhesives* 2006, 26, 304.
16. Zhou, M.; Qiu, X.; Yang, D.; Wang, W. *Energy Conversion Manage* 2007, 48, 204.
17. Kalenda, P. *Pigments Resin Technol* 2002, 31, 284.
18. Lozano, M.; Blanco, M. D.; Olmo, R.; Lozano, R.; Teijon, J. M. *Polym Int* 1999, 42, 245.
19. Singh, M. *J Biochem Biophys Methods* 2006, 67, 151.
20. Wang, N.; Yu, J.; Ma, X. F. *Polym Compos* 2008, 29, 551.
21. Kholodenko, A. L.; Douglas, J. F. *Phys Rev E* 1995, 51, 1081.
22. Singh, M.; Gupta, S. *Synth Commun* 2008, 38, 2898.
23. Singh, M.; Yadav, D.; Yadav, R. K. *J Appl Polym Sci* 2008, 110, 2601.